Article:
Xu, Z. Y., Grzywacz, R., Gottardo, A. et al. (49 more authors) (2024) Compound-Nucleus and Doorway-State Decays of β-Delayed Neutron Emitters 51,52,53K. Physical Review Letters. 042501. ISSN: 1079-7114

https://doi.org/10.1103/PhysRevLett.133.042501

Compound-Nucleus and Doorway-State Decays of β-Delayed Neutron Emitters ^{51,52,53}K

Z. Y. Xu,[1] R. Grzywacz,[1,2] A. Gottardo,[3,4] M. Madurga,[1] I. M. Alonso,[5] A. N. Andreyev,[6,7] G. Benzoni,[8] M. J. G. Borge,[5] T. Cap,[9] C. Costache,[10] H. De Witte,[11] B. I. Dimitrov,[12,13] J. E. Escher,[14] A. Fijalkowska,[15,16] L. M. Fraile,[17] S. Franchoo,[3] H. O. U. Fynbo,[18] B. C. Gonsalves,[19] C. J. Gross,[2] L. J. Harkness-Brennan,[20] J. Heideman,[1] M. Huyse,[11] D. S. Judson,[20] T. Kawano,[21] T. T. King,[1,2] S. Kisyov,[10,22] K. Kolos,[23] A. Korgul,[16] I. Lazarus,[24] R. Lică,[25,10] M. L. Liu,[26] L. Lynch,[25] N. Marginean,[10] R. Marginean,[10] C. Mazzocchi,[16] D. Mengoni,[27,28] C. Mihai,[10] A. I. Morales,[29] R. D. Page,[20] J. Pakarinen,[30,31] S. V. Paulauskas,[1] A. Perea,[5] M. Piersa-Siłkowska,[16,25] Zs. Podolyák,[32] Ch. Sotty,[10] S. Taylor,[1] O. Tengblad,[5] P. Van Duppen,[11] V. Vedia,[17] D. Verney,[3] N. Warr,[33] and C. X. Yuan[26]

[1]*Department of Physics and Astronomy, University of Tennessee, Knoxville, Tennessee 37996, USA*
[2]*Physics Division, Oak Ridge National Laboratory, Oak Ridge, Tennessee 37831, USA*
[3]*Université Paris-Saclay, IJCLab, CNRS/IN2P3, F-91405 Orsay, France*
[4]*INFN, Laboratori Nazionali di Legnaro, I-35020 Legnaro, Padova, Italy*
[5]*Instituto de Estructura de la Materia, IEM-CSIC, Serrano 113 bis, E-28006 Madrid, Spain*
[6]*School of Physics, Engineering and Technology, University of York, North Yorkshire YO10 5DD, United Kingdom*
[7]*Advanced Science Research Center, Japan Atomic Energy Agency, Tokai, Ibaraki 319-1195, Japan*
[8]*Istituto Nazionale di Fisica Nucleare, Milano, I-20133 Milano, Italy*
[9]*National Centre for Nuclear Research, Pasteura 7, 02-093 Warsaw, Poland*
[10]*Horia Hulubei National Institute for Physics and Nuclear Engineering, RO-077125 Bucharest, Romania*
[11]*KU Leuven, Instituut voor Kern- en Stralingsfysica, B-3001 Leuven, Belgium*
[12]*Faculty of Physics, Sofia University "St Kliment Ohridski," 1164 Sofia, Bulgaria*
[13]*Bulgarian Academy of Sciences, Institute for Nuclear Research and Nuclear Energy, 1784 Sofia, Bulgaria*
[14]*Nuclear and Chemical Sciences Division, Lawrence Livermore National Laboratory, Livermore, California 94551, USA*
[15]*Department of Physics and Astronomy, Rutgers University, New Brunswick, New Jersey 08903, USA*
[16]*Faculty of Physics, University of Warsaw, PL 02-093 Warsaw, Poland*
[17]*Grupo de Física Nuclear and IPARCOS, Facultad de CC. Físicas, Universidad Complutense de Madrid, E-28040 Madrid, Spain*
[18]*Department of Physics and Astronomy, Aarhus University, DK-8000 Aarhus C, Denmark*
[19]*Department of Physics, University of Helsinki, P.O. Box 43, FI-00014 University of Helsinki, Finland*
[20]*Department of Physics, Oliver Lodge Laboratory, University of Liverpool, Liverpool L69 7ZE, United Kingdom*
[21]*Theoretical Division, Los Alamos National Lab, Los Alamos, New Mexico 87545, USA*
[22]*Lawrence Berkeley National Laboratory, Berkeley, California 94720, USA*
[23]*Lawrence Livermore National Laboratory, Livermore, California 94550, USA*
[24]*STFC Daresbury, Daresbury, Warrington WA4 4AD, United Kingdom*
[25]*ISOLDE, EP Department, CERN, CH-1211 Geneva, Switzerland*
[26]*Sino-French Institute of Nuclear Engineering and Technology, Sun Yat-sen University, Zhuhai 519082, China*
[27]*Istituto Nazionale di Fisica Nucleare, Sezione di Padova, I-35131, Padova, Italy*
[28]*Dipartimento di Fisica e Astronomia, Universitá di Padova, I-35131 Padova, Italy*
[29]*Instituto de Física Corpuscular, CSIC-Universidad de Valencia, E-46071, Valencia, Spain*
[30]*University of Jyväskylä, Department of Physics, P.O. Box 35, FI-40014, Jyväskylä, Finland*
[31]*Helsinki Institute of Physics, University of Helsinki, P.O. Box 64, FIN-00014, Helsinki, Finland*
[32]*Department of Physics, University of Surrey, Guildford GU2 7XH, United Kingdom*
[33]*Institut für Kernphysik, Universität zu Köln, 50937 Köln, Germany*

(Received 12 December 2023; revised 11 April 2024; accepted 20 May 2024; published 22 July 2024)

We investigated decays of ^{51,52,53}K at the ISOLDE Decay Station at CERN in order to understand the mechanism of the β-delayed neutron-emission (βn) process. The experiment quantified neutron and γ-ray emission paths for each precursor. We used this information to test the hypothesis, first formulated by Bohr in 1939, that neutrons in the βn process originate from the structureless "compound nucleus." The data are consistent with this postulate for most of the observed decay paths. The agreement, however, is surprising because the compound-nucleus stage should not be achieved in the studied β decay due to

insufficient excitation energy and level densities in the neutron emitter. In the ^{53}K βn decay, we found a preferential population of the first excited state in ^{52}Ca that contradicted Bohr's hypothesis. The latter was interpreted as evidence for direct neutron emission sensitive to the structure of the neutron-unbound state. We propose that the observed nonstatistical neutron emission proceeds through the coupling with nearby doorway states that have large neutron-emission probabilities. The appearance of "compound-nucleus" decay is caused by the aggregated small contributions of multiple doorway states at higher excitation energy.

DOI: 10.1103/PhysRevLett.133.042501

Introduction—The β-delayed neutron emission discovered by Roberts [1] was explained by Bohr [2] as a two-step sequential decay process that occurs for very neutron-rich nuclei. β decays of the precursors populate highly excited, neutron-unbound states in the intermediate nuclei, which decay via neutron emission. Understanding the foundations of βn emission is crucial in diverse areas of nuclear science, from nuclear reactors to astrophysical nucleosynthesis [3–10], and will inform the delayed particle emission on the proton-rich side. However, because of the challenges in both experiment and theory, our knowledge of this significant process is far from satisfactory.

Because of the complicated nature of the βn emission, theoretical descriptions have long been relying on Bohr's hypothesis of the compound nucleus (CN) [11], from which the neutron emission depends only on its spin, parity, and excitation energy and is independent of the formation process [12]. Early studies attempted to compare the predictions made by statistical-model calculations to measured energy spectra of neutrons emitted from fission-fragment precursors and to the probabilities populating the excited states in residues [13–17]. The observed discrepancies led to the conclusion that nuclear structure affects βn emission. However, those analyses employed too simple or unrealistic assumptions regarding the β-decay process. Currently, the established theoretical framework calculates the βn emission in two steps. First, the β-strength distribution is computed using microscopic models such as the quasiparticle random phase approximation or the nuclear shell model. Then, neutron emission from the states above the neutron separation energy (S_n) in the daughter is evaluated with the statistical Hauser-Feshbach theory and the implicit assumption of the CN; see Refs. [18–20]. Transmission coefficients are calculated using a chosen optical model potential (OMP). The approach has been employed in predicting gross β-decay properties such as the inclusive βn probabilities (P_n), achieving some agreement with the experimental data for known medium- and heavy-mass nuclei [10,18–21]. Only recently has the underlying CN assumption been questioned again based on experimental data: it seems that the observed neutron emissions from excited states in ^{134}Sn are related to the structure of the states populated in the decay of the parent nucleus ^{134}In [22]. If proven more broadly, a revision of β-delayed neutron-emission models is needed with consequences in power-generation and astrophysical applications.

Owing to the developments of intense radioactive ion beams and the combination of high-resolution γ and neutron spectrometers, it becomes possible to comprehensively study the βn process for a much broader spectrum of nuclei. Precursors with much larger β-decay energies (Q_β) and decreasing S_n can now be accessed. These advances allow for investigating and, if necessary, revising the CN hypothesis in β decay. In addition, the validity of the choice of OMP could be probed for very exotic nuclei where other methods are not available.

In this Letter, we report on measurements of the βn branching ratios in the neutron-rich ^{51,52,53}K (proton number $Z = 19$, neutron number $N = 32$, 33, 34, respectively) isotopes, which reside near the proton $Z = 20$ and neutron $N = 32$, 34 closed shells [23–25]. Since the nuclear level densities (NLD) in their daughter nuclei are anticipated to be low, they are expected to be candidates where the CN hypothesis is broken, similar to the ^{134}In case [22]. Indeed, we observed a few neutron-emitting states in ^{53}Ca exhibiting nonstatistical behavior, which is interpreted as the configuration mixing with doorway states—the states having large neutron-emission probabilities [22]. More importantly, we show, for the first time, that the statistical model can reproduce experimental data well after normalizing the exclusive neutron branching ratios with β-feeding strength. However, this occurs in an energy regime where the low NLD in the neutron-emitting nucleus raises significant doubts about the application of Bohr's CN assumption. Furthermore, we present that an OMP with a standard range of parameters can describe neutron-emission transmission coefficients. This unexpected, apparent CN decay could be explained by the absence of nearby doorway states and caused by the contributions from small and random configurations at higher excitation energies. It could be the evidence for possible chaotic effects coexisting with regular motion at low-energy nuclear excitations, which further impact the descriptions of other nuclear processes where the CN assumption is used [26–29].

Experiment and results—The Isotope Separator On-Line (ISOLDE) facility at CERN [30] produced the neutron-rich ^{51,52,53}K isotopes in fission. The 1.4-GeV proton beam from the Proton Synchrotron Booster bombarded a uranium

carbide target with an average current of 2 μA. Following surface ionization, the General Purpose Separator [30] selected potassium isotopes of interest at mass number 51, 52, and 53 respectively. The radioactive ion beam was delivered to the ISOLDE Decay Station (IDS), where the beam was implanted on a moveable tape system. The hybrid detection system at IDS consisted of two plastic β scintillators, four high-purity Ge clovers, and 26 VANDLE neutron detectors modules [31]. More details of the setup can be found in Ref. [32].

Figure 1 presents the neutron time-of-flight (TOF) spectra taken in coincidence with the β decays of ^{51,52,53}K. The top row shows the full neutron-singles spectra. The middle and bottom ones are generated requiring additional coincidence with the γ-ray de-excitations from the first and second excited states in their respective βn residues. In deconvoluting these spectra, we employed the neutron response function given in Ref. [32]. Our procedure for obtaining the β-feeding probabilities (I_β) and βn branching ratios ($I_{\beta n}$) is as follows. We start with a series of neutron-unbound states in the daughter, with the kth state at E_x^k excitation energy. Then, we generate all possible neutron peaks associated with the state according to the low-lying states in residues [33]. The neutron energies (intensities) are denoted as $E_n^{k\to l}$ ($I_n^{k\to l}$), where l stands for the lth state in the residue. With known S_n and E_x^l, all associated $E_n^{k\to l}$ can be computed from a given E_x^k. We extract E_x^k and their $I_n^{k\to l}$ simultaneously from a χ^2 analysis fitting all together the neutron-singles and neutron-γ coincidence spectra. In Fig. 1, the resultant response functions (magenta) are deconvoluted into individual neutron peaks feeding the ground (red), first (black), second (blue), and higher (green) excited states in residues. Lastly, we obtained $I_{\beta n}(k\to l) = I_n^{k\to l}/N_\beta$ and $I_\beta(k) = \sum_l I_{\beta n}(k\to l)$, with N_β being the number of β decays detected by the β scintillators.

While the extracted I_β and its related physics will be presented elsewhere [34], this Letter focuses on neutron emissions from the daughter. Figure 2 plots the fraction of $I_{\beta n}(k\to l)$ with respect to the β-feeding $I_\beta(k)$ as a function of the daughter's excitation energy. This variable decouples itself from the fluctuation of the preceding β-decay feeding and reflects how the neutron emissions favor the low-lying states in residues from a given unbound state. Although any state lying below E_x^k in residue can be populated, its intensity drops quickly with rising excitation energy. This can be seen in Fig. 1 where the green neutron peaks feeding the states higher than the second excited state in residue are extremely weak and almost invisible in the deconvolution. We only accounted for the residue states with feeding strength above our experimental limit in extracting $I_\beta(k)$. Those states are drawn as inserts in the top row of Fig. 2. Similarly, only the fractions to the ground, first, and

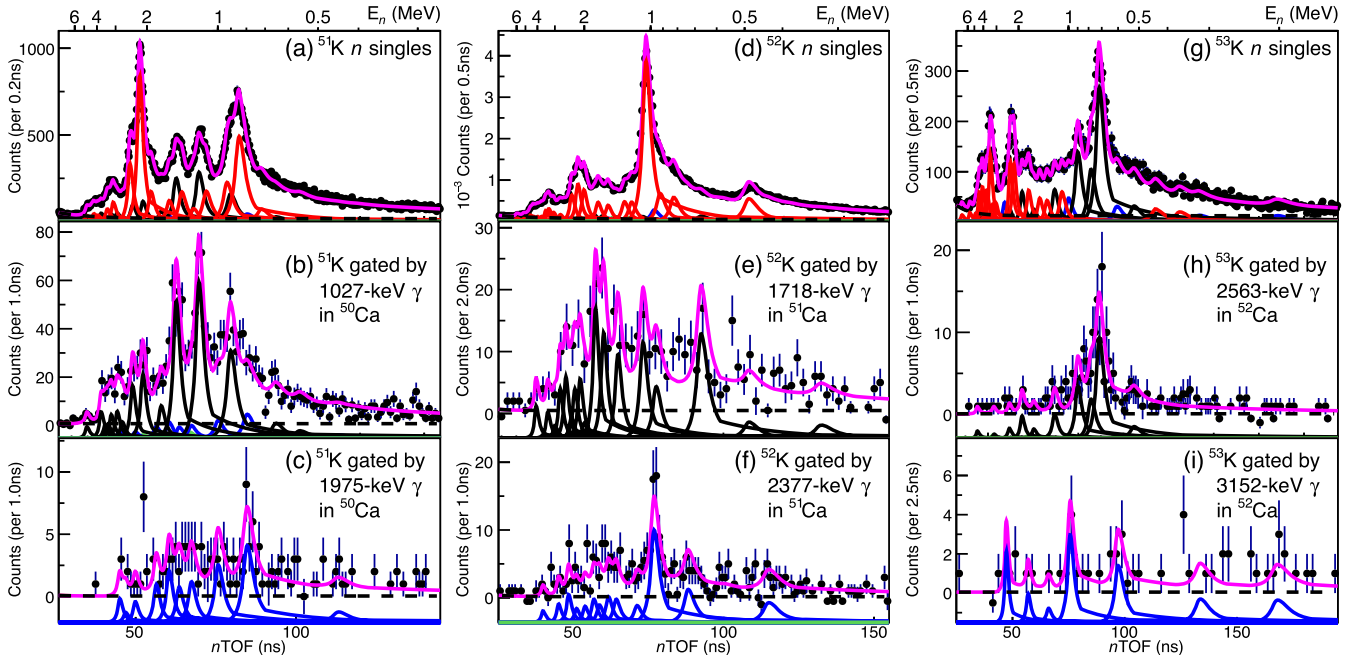

FIG. 1. Neutron TOF spectra following the ^{A}K β decays, with $A = 51$ (left), 52 (middle), and 53 (right). The top row (a, d, and g) presents the full neutron TOF spectra (neutron singles) of each isotope, whereas the center (b, e, and h) and bottom (c, f, and i) rows show the neutron spectra coinciding with the γ de-excitations from the first and second excited states in $^{A-1}$Ca, respectively. The spectra are fitted by the neutron response functions (magenta), which can be deconvoluted into individual neutron-emission peaks. The neutron emissions feeding the ground, first, and second excited state in $^{A-1}$Ca are drawn in red, black, and blue, respectively. Feedings to any higher excited states, generally too weak to be visible in the plots, are shown in green. The individual peaks have been shifted down on the y axis for visualization purposes.

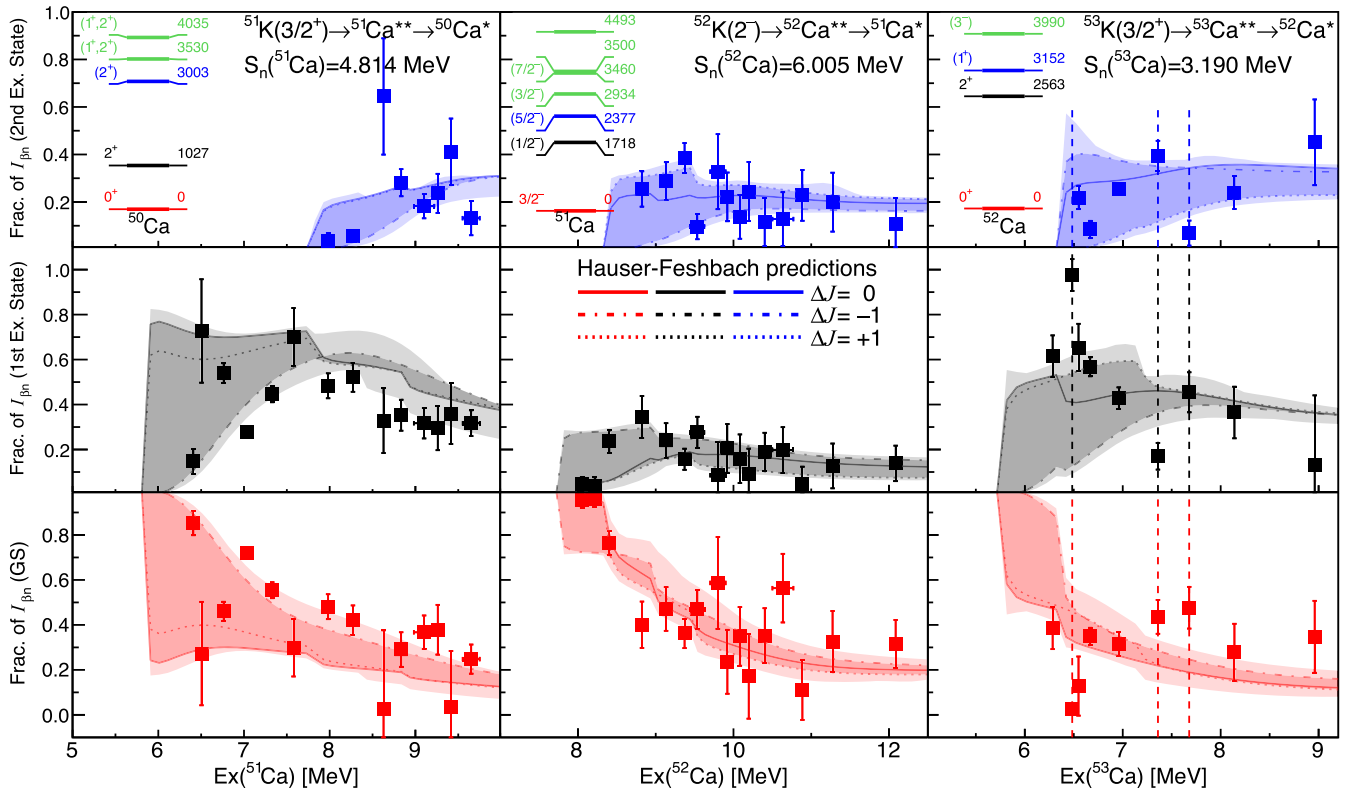

FIG. 2. Exclusive βn branching ratios of ^{A}K, with $A = 51$ (left), 52 (middle), and 53 (right). The x axis is the excitation energy of the ^{A}Ca** states (** stands for neutron unbound) populated in β decay, while the y axis is the fraction of $I_{\beta n}$ from that state to the ground (bottom, red), first (center, black), and second (top, blue) excited states in $^{A-1}$Ca* (* means either the ground or low-lying excited state). The $^{A-1}$Ca states involved in the analysis are shown in the partial level scheme. The dark color bands represent the Hauser-Feshbach predictions covering all spin scenarios in the GT decay, including $\Delta J = 0$ (solid curves), -1 (dash-dotted curves), and $+1$ (dotted curves). The light color bands indicate additional uncertainty from OMP (see main text). The experimental data that strongly deviate from theory (more than 3σ of combined experimental and theoretical uncertainties) are highlighted by the vertical dashed lines.

second excited states are discussed in more details in the following sections.

Comparison with statistical decay—We employed statistical model calculations using the Hauser-Feshbach (HF) formalism [35] to compare with our data. The model inputs, such as the excitation energies, spins, and parities of residue states, are taken from literature whenever available [36]. Starting from the ^{51}K ($J^\pi = 3/2^+$), ^{52}K ($J^\pi = 2^-$), and ^{53}K ($J^\pi = 3/2^+$) ground states [33,37], we considered three possible spin scenarios in the daughters according to the selection rule of allowed Gamow-Teller (GT) transitions ($\Delta J = 0, \pm 1$), which are the major β-decay modes populating the observed neutron-unbound states [34]. The results are shown in Fig. 2. Since an observed peak may consist of multiple states due to the finite energy resolution, we draw the dark color bands between the upper and lower limits of different spin scenarios to simulate the averaging effects. Furthermore, we studied the sensitivity of our results to the OMP being used. The nominal calculations were done with the Koning-Delaroche (KD) OMP [38]. Then, we varied the parameters in the KD OMP coherently following the procedure outlined in Ref. [39]. The impact on the $I_{\beta n}$ fractions is indicated by the outer bands in light color.

The most striking feature in Fig. 2 is the overall good agreement between the experimental data and the model predictions across the measured energy range, even though ^{51,52,53}Ca are considered to be semi- or doubly magic nuclei with low NLD. This was corroborated by our large-scale shell-model (LSSM) calculations [40,41] with the sdpf-mu interaction [42], which yield the NLD of ^{51,52,53}Ca 10–20 states per MeV in the energy range of interest. These values are 5–20 times smaller than the Gilbert-Cameron formula prediction [43], which was used to provide NLD for the statistical calculations. The agreement in Fig. 2 suggests a nucleus with considerably lower NLD than what the HF model assumes may undergo apparent statistical neutron emission if there is no other direct channel available. It is also noteworthy that for cases where the data agree with the statistical model, this comparison allows for model-dependent spin assignments for those neutron-unbound states. Examples are the states at 7.3 MeV in ^{51}Ca ($J = 1/2$), 9.5 MeV in ^{52}Ca ($J = 1$), and 7 MeV in ^{53}Ca ($J = 3/2$).

Doorway-state decay—In Fig. 2, there are a few outliers in ^{53}Ca, highlighted by the vertical dashed lines, whose decays do not follow statistical neutron emission even if the theoretical uncertainty from the OMP is included. The strongest deviation is seen at 6.48 MeV, which is about 3.29 (0.73) MeV above the ground (first excited) state of ^{52}Ca. Because of the huge phase space, the HF calculation predicts a significant amount of ground-state population (∼40%), which contradicts the preferential feeding to the first excited state observed experimentally (> 90%). Between 7 and 8 MeV, there are two more states manifesting ground-state feedings that are stronger than the HF model predictions.

Recently, we suggested that βn emission may involve a doorway state—the state having strong spectroscopic overlap with the residue at low energy [22]. In ^{53}Ca, a doorway state can be written as $n_j^\dagger \oplus |^{52}\mathrm{Ca}^*\rangle$, where ^{52}Ca* stands for a low-lying state of the ^{52}Ca core and n_j a neutron on the single-particle orbital j outside. To mix with the states in ^{53}Ca populated in the GT decay, of which $J^\pi = 1/2^+$, $3/2^+$, or $5/2^+$, the parities of doorway states need to be positive. On the other hand, the low-lying states in ^{52}Ca have positive parities as well, restricting the parity of the neutron orbital j to be positive and excluding the configurations with pf orbitals. The lowest energy candidates fulfilling the requirement are the $\nu g_{9/2}$ and $\nu d_{5/2}$ orbitals beyond $N = 40$; see Fig. 3 (left). Interestingly, if j is $\nu g_{9/2}$, only a ^{52}Ca core at $J^\pi = 2^+$ allows mixing between a state populated in β decay and a doorway state, both of which have $J^\pi = 5/2^+$. Such mixing will drive a significant amount of neutron emission to the 2^+ state, as observed for the 6.48-MeV state in the ^{53}K decay.

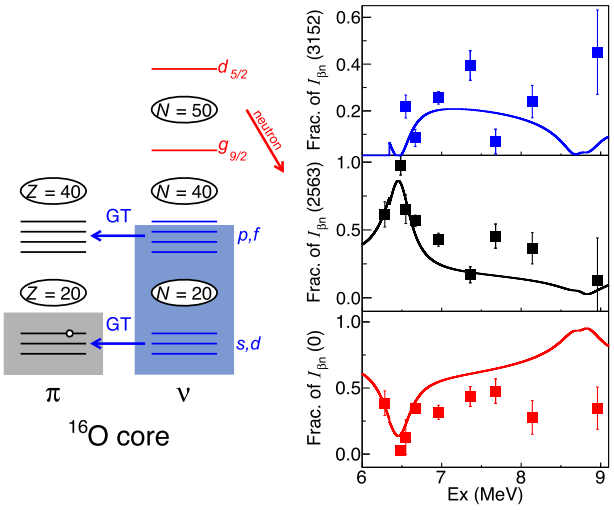

FIG. 3. Left: schematic drawing of the single-particle orbitals in ^{53}K relevant to the βn emission. The gray (blue) box represents the occupied proton (neutron) orbitals below the Fermi surface. Outside the ^{16}O core, the neutron orbitals contributing to the GT decay and the doorway-state neutron emission are shown in blue and red, respectively. See text for more details. Right: calculated fractions of $I_{\beta n}$ following the ^{53}K decay based on the doorway states with $J = 5/2$ (solid lines), together with the experimental data (solid square). Red, black, and blue represent the feeding to the ground, first, and second excited states of ^{52}Ca, respectively.

Unlike $\nu g_{9/2}$, an n_j with $\nu d_{5/2}$ allows for various coupling schemes of the doorway states. Quantitative interpretation of their $I_{\beta n}$ requires developing a microscopic model capable of calculating the configuration mixing between the states from GT transitions and doorway states, which is beyond the scope of this Letter. Instead, we invoke a simple model introduced in Ref. [22]. This model relies on the realization that the spectroscopic overlaps between states in the residue and the neutron-emitting states populated in β decay are minimal. Here, the LSSM predicts spectroscopic factors below 10^{-3}. In our model, the neutron emission can be described as due to configuration mixing with tails of neutron-emitting resonances. In brief, we write the energy profile of the broad doorway state in the form of a normalized Breit-Wigner function. Its full width is determined as the sum of partial decay widths, with the latter defined as the neutron transmission coefficient to a lower residue state scaled by the spectroscopic factor for single-neutron removal. The fraction of $I_{\beta n}$ of the doorway state is simply the ratio of the partial to total width. For the states from β decay residing at E_{ex}^{β}, the fractions of $I_{\beta n}$ are obtained as the weighted average of the nearby doorway states. Given the centroid energy of doorway states E_{ex}^{dw}, the weights are computed as their amplitudes at E_{ex}^{β}. We calculated the neutron transmission coefficients with the KD OMP. The E_{ex}^{dw} and related spectroscopic factors in ^{53}Ca are given by LSSM in the sdpf-g9d5 model space as shown in Fig. 3 (left). The single- and two-body matrix elements are obtained as a subset of the sdpf-sdg interaction [44]. In the model space, the spin of the doorway states that can decay to all three lowest-lying states of ^{52}Ca, which have $J = 0$, 2, and 1, respectively, is constrained to $J = 5/2$. In spite of their limited precision, the new calculations reproduce the trends reasonably well, suggesting the doorway-state decay is indeed a promising solution to understand βn emission when it deviates from the HF model.

Lastly, we note the existence of doorway states cannot be completely excluded in the ^{51,52}K decays. There are a few candidates, such as the states around 9 MeV in ^{51}Ca and 8.8 MeV in ^{52}Ca, not fully following the HF prediction with a given spin or average of spins. However, the deviation is only between 1- and 3-σ, preventing us from drawing strong conclusions. Future measurements with either more statistics or definite spin assignment will be helpful in identifying these states in ^{51,52}Ca or finding more doorway-state decays in ^{53}Ca.

Conclusions and perspectives—In summary, we studied the βn branching ratios of ^{51,52,53}K at IDS using high-resolution γ-ray and neutron TOF spectroscopy. The

experimental results show overall good agreement with the statistical model predictions, with only a few clear deviations in the ^{53}K decay. We conclude that despite the low NLD, neutron-rich ^{51,52,53}K nuclei follow mostly statistical βn emission. However, when an open channel such as a doorway-state decay appears in the relevant energy region, strong deviations from statistical decay emerge locally. An advanced theoretical framework that includes nuclear shell structure or is based on the time-dependent methods is desired to fully understand the βn process across the nuclear chart [45,46].

Acknowledgments—We acknowledge the support of the ISOLDE Collaboration and technical teams. The authors thank Dr. Sota Yoshida for valuable discussions and sharing the sdpf-sdg effective interaction [44]. This project was supported by the European Unions Horizon 2020 research and innovation programme under the Grant Agreement No. 654002 (ENSAR2) and the Marie Skłodowska-Curie Grant Agreement No. 101032999 (BeLaPEx), by the Office of Nuclear Physics, U.S. Department of Energy under Award No. DE-FG02-96ER40983 (UTK) and DE-AC05-00OR22725 (ORNL), by the auspices of the National Nuclear Security Administration of the U.S. Department of Energy at Los Alamos National Laboratory under Contract No. 89233218CNA000001, by the auspices of the U.S. Department of Energy at Lawrence Livermore National Laboratory under Contract No. DE-AC52-07NA27344, by the National Nuclear Security Administration under the Stewardship Science Academic Alliances program through DOE Award No. DE-436NA0003899, No. DE-NA0002132, and No. DE-NA0004068, by the Romanian IFA grant CERN/ISOLDE and Nucleu Project No. PN 23 21 01 02, by the Research Foundation Flanders (FWO, Belgium) and by BOF KU Leuven (C14/22/104), by the German BMBF under Contracts No. 05P18PKCIA and No. 05P21PKCI1 in Verbundprojekte 05P2018 and 05P2021, by the UK Science and Technology Facilities Research Council (STFC) of the UK Grants No. ST/R004056/1, No. ST/P004598/1, No. ST/P003885/1, No. ST/V001027/1, and No. ST/V001035/1, by the Guangdong Major Project of Basic and Applied Basic Research under Grant No. 2021B0301030006, by the Polish National Science Center under Grant No. 2020/39/B/ST2/02346, by the Polish Ministry of Education and Science under Contract No. 2021/WK/07, by Spanish MCIN/AEI/10.13039/501100011033 under Grants No. PGC2018-093636-B-I00, No. RTI2018-098868-B-I00, No. PID2019-104390 GB-I00, No. PID2019-104714 GB-C21, No. PID2021-126998OB-I00, and No. PID2022-140162NB-I00, by Generalitat Valenciana, Conselleria de Innovación, Universidades, Ciencia y Sociedad Digital under Grant No. CISEJI/2022/25, and by Universidad Complutense de Madrid (Spain) through Grupo de Física Nuclear (910059). The shell-model LD were calculated with KSHELL [47]. The doorway-state energies and spectroscopic factors were obtained from NuShellX@MSU [48]. The Hauser-Feshbach calculations were done using the BeoH code [49].

[1] R. B. Roberts, R. C. Meyer, and P. Wang, Phys. Rev. **55**, 510 (1939).
[2] N. Bohr and J. A. Wheeler, Phys. Rev. **56**, 426 (1939).
[3] G. R. Keepin, T. F. Wimett, and R. K. Zeigler, Phys. Rev. **107**, 1044 (1957).
[4] K. Farouqi, K.-L. Kratz, B. Pfeiffer, T. Rauscher, F.-K. Thielemann, and J. W. Truran, Astrophys. J. **712**, 1359 (2010).
[5] K. Miernik, Phys. Rev. C **88**, 041301(R) (2013).
[6] K.-L. Kratz, AIP Conf. Proc. **1645**, 109 (2015).
[7] R. Caballero-Folch *et al.*, Phys. Rev. Lett. **117**, 012501 (2016).
[8] A. Algora, J. L. Tain, B. Rubio, M. Fallot, and W. Gelletly, Eur. Phys. J. A **57**, 85 (2021).
[9] G. G. Kiss *et al.*, Astrophys. J. **936**, 107 (2022).
[10] V. H. Phong *et al.*, Phys. Rev. Lett. **129**, 172701 (2022).
[11] N. Bohr, Nature (London) **137**, 344 (1936).
[12] P. Hansen and B. Jonson, Beta delayed particle emission from neutron rich nuclei, in *Particle Emission from Nuclei*, Vol. 3, edited by M. Ivascu and D. Poenaru (CRC Press, Boca Raton, Florida, 1989), pp. 157–201.
[13] H. Franz, J. V. Kratz, K. L. Kratz, W. Rudolph, G. Herrmann, F. M. Nuh, S. G. Prussin, and A. A. Shihab-Eldin, Phys. Rev. Lett. **33**, 859 (1974).
[14] A. Shihab-Eldin, W. Halverson, F. Nuh, S. Prussin, W. Rudolph, H. Ohm, and K. Kratz, Phys. Lett. **69B**, 143 (1977).
[15] S. Prussin, Z. Oliveira, and K.-L. Kratz, Nucl. Phys. **A321**, 396 (1979).
[16] H. V. Klapdor and C. O. Wene, J. Phys. G **6**, 1061 (1980).
[17] P. Hoff, Nucl. Phys. **A359**, 9 (1981).
[18] T. Kawano, P. Möller, and W. B. Wilson, Phys. Rev. C **78**, 054601 (2008).
[19] P. Möller, M. Mumpower, T. Kawano, and W. Myers, At. Data Nucl. Data Tables **125**, 1 (2019).
[20] F. Minato, T. Marketin, and N. Paar, Phys. Rev. C **104**, 044321 (2021).
[21] R. Yokoyama *et al.*, Phys. Rev. C **100**, 031302 (2019).
[22] J. Heideman *et al.* (IDS Collaboration), Phys. Rev. C **108**, 024311 (2023).
[23] F. Wienholtz *et al.*, Nature (London) **498**, 346 (2013).
[24] D. Steppenbeck *et al.*, Nature (London) **502**, 207 (2013).
[25] S. Chen *et al.*, Phys. Rev. Lett. **123**, 142501 (2019).
[26] V. Zelevinsky, Nucl. Phys. **A553**, 125 (1993).
[27] H. A. Weidenmueller, Comments Nucl. Part. Phys. **16**, 199 (1986).
[28] V. Sokolov and V. Zelevinsky, Ann. Phys. (N.Y.) **216**, 323 (1992).
[29] A. Spyrou, S. N. Liddick, A. C. Larsen, M. Guttormsen, K. Cooper, A. C. Dombos, D. J. Morrissey, F. Naqvi, G. Perdikakis, S. J. Quinn, T. Renstrøm, J. A. Rodriguez,

A. Simon, C. S. Sumithrarachchi, and R. G. T. Zegers, Phys. Rev. Lett. **113**, 232502 (2014).
[30] R. Catherall, W. Andreazza, M. Breitenfeldt, A. Dorsival, G. J. Focker, T. P. Gharsa, G. T. J, J.-L. Grenard, F. Locci, P. Martins, S. Marzari, J. Schipper, A. Shornikov, and T. Stora, J. Phys. G **44**, 094002 (2017).
[31] W. Peters *et al.*, Nucl. Instrum. Methods Phys. Res., Sect. A **836**, 122 (2016).
[32] Z. Y. Xu *et al.*, Phys. Rev. C **108**, 014314 (2023).
[33] F. Perrot *et al.*, Phys. Rev. C **74**, 014313 (2006).
[34] A. Gottardo *et al.* (to be published).
[35] W. Hauser and H. Feshbach, Phys. Rev. **87**, 366 (1952).
[36] ENSDF database as of April 12th, 2023, http://www.nndc.bnl.gov/ensarchivals.
[37] J. Papuga, M. L. Bissell, K. Kreim, K. Blaum, B. A. Brown, M. De Rydt, R. F. Garcia Ruiz, H. Heylen, M. Kowalska, R. Neugart, G. Neyens, W. Nörtershäuser, T. Otsuka, M. M. Rajabali, R. Sánchez, Y. Utsuno, and D. T. Yordanov, Phys. Rev. Lett. **110**, 172503 (2013).
[38] A. Koning and J. Delaroche, Nucl. Phys. **A713**, 231 (2003).
[39] C. D. Pruitt, J. E. Escher, and R. Rahman, Phys. Rev. C **107**, 014602 (2023).
[40] N. Shimizu, Y. Utsuno, Y. Futamura, T. Sakurai, T. Mizusaki, and T. Otsuka, Phys. Lett. B **753**, 13 (2016).
[41] J. Chen, M. Liu, C. Yuan, S. Chen, N. Shimizu, X. Sun, R. Xu, and Y. Tian, Phys. Rev. C **107**, 054306 (2023).
[42] Y. Utsuno, T. Otsuka, B. A. Brown, M. Honma, T. Mizusaki, and N. Shimizu, Phys. Rev. C **86**, 051301(R) (2012).
[43] A. Gilbert and A. G. W. Cameron, Can. J. Phys. **43**, 1446 (1965).
[44] S. Yoshida, Y. Utsuno, N. Shimizu, and T. Otsuka, Phys. Rev. C **97**, 054321 (2018).
[45] L. Guo, D. Lacroix, N. Schunck, C. Simenel, and P. Stevenson, Front. Phys. **8**, 629889 (2021).
[46] O. C. Gorton, C. W. Johnson, and J. E. Escher, Eur. Phys. J. Web Conf. **284**, 03013 (2023).
[47] N. Shimizu, T. Mizusaki, Y. Utsuno, and Y. Tsunoda, Comput. Phys. Commun. **244**, 372 (2019); code is available at https://sites.google.com/a/cns.s.u-tokyo.ac.jp/kshell.
[48] B. Brown and W. Rae, Nucl. Data Sheets **120**, 115 (2014).
[49] S. Okumura, T. Kawano, P. Jaffke, P. Talou, and S. Chiba, J. Nucl. Sci. Technol. **55**, 1009 (2018).